Journal of Alloys and Compounds 509 (2011) 6408–6413

Contents lists available at ScienceDirect

Journal of Alloys and Compounds

journal homepage: www.elsevier.com/locate/jallcom

N, Fe and WO_3 modified TiO_2 for degradation of formaldehyde

Haixia Tong[a,b,*], Li Zhao[c], Dan Li[a,b], Xiongfei Zhang[b]

[a] Chemical and Biologic Engineering Institute, Changsha University of Science and Technology, Hunan Province Key Laboratory of Materials Protection for Electric Power and Transportation, Changsha 410114, Hunan, China
[b] College of Metallurgical Science and Engineering, Central South University, Changsha 410083, Hunan, China
[c] College of Chemistry and Chemical Engineering, Nanjing University, Nanjing 210093, Jiangsu, China

ARTICLE INFO

Article history:
Received 6 November 2010
Received in revised form 10 March 2011
Accepted 13 March 2011
Available online 21 March 2011

Keywords:
N–Fe co-doping
WO_3 compounded
Photocatalysis
Formaldehyde

ABSTRACT

Butyltitanate, ethanol and glacial acetic acid were chosen as titanium source, solvent and chelating agent, respectively, via a sol–gel method combined impregnation method to prepare N, Fe co-doped and WO_3 compounded photocatalyst TiO_2 powder. The synthesized products were characterized by X-ray diffraction (XRD), diffuse reflectance UV–Vis spectra (UV-DRS), scanning electron microscopy (SEM) and X-ray photoelectron spectroscopy (XPS). Photocatalytic degradation of formaldehyde was employed to investigate the catalytic activity. The results show that the degradation rate is 77.61% in 180 min under UV light irradiation when the concentration of N is fixed on, and the optimum proportioning ratio of n(Fe):n(W):n(Ti) is 0.5:2:100.

1. Introduction

The treatment of industrial waste waters for removing organic pollutants is nowadays a very important aspect of environmental technology. Consequently a growing interest in heterogeneous photocatalysis, as an advanced oxidation technique, has been developed [1,2]. The use of nanocrystalline semiconductors as photocatalysts, to initiate interfacial redox reactions, have generated great interest, due to their unique physicochemical properties, caused by their nanosized dimensions and large surface/volume ratios.

In this context, among of various photocatalysts including TiO_2, ZnO_2, WO_3, CdS, ZnS, $SrTiO_3$, and Fe_2O_3, TiO_2 has been investigated as the most promising photocatalyst for the treatment of pollutants, from water and air, since it has a reasonable photoactivity under ultraviolet light irradiation (anatase, Eg = 3.2 eV), and is nontoxic, water insoluble, and comparatively inexpensive.

However, as a wide bandgap semiconductor, TiO_2 can absorb only the UV light of solar energy, which limits their practical application. At the present time, many researches are carried out in order to substitute the UV light by visible light or the sunlight. This will reduce the cost of the photodegradation process especially for industrial scale applications. Using dopants that can be incorporated in TiO_2 lattice is one of the methods used to reach this goal [3–11]. Results show that doping TiO_2 with transition metals or non-metal elements (S, N, C and F) increases its photocatalytic activity [7–11]. It is reported that doped ions can enhance the intensity of absorption in the UV–Vis light region and make a red shift in the band gap transition of the doped TiO_2 samples. For example in the case of Fe–TiO_2 sample, Fe ions play two roles: as a photo-generated hole or a photo-generated electron trap which reduce the hole–electron recombination, or as a mediator of the transfer of interfacial charge [7,11]. However, there is a controversy on the effect of metals ions on the photocatalytic activity of TiO_2. Other authors show a decrease of photocatalytic activity of the doped catalysts [12–15]. The amount of the metal ions that can be incorporated in TiO_2 lattice is also a controversial matter [7,9,10].

Some studies have also shown that semiconductor compounding is beneficial to the separation of the photo-electrons and holes, which can enhance the photocatalytic efficiency. For example, Zhang et al. [16] reported that the speed of the photocatalytic degradation of methylene blue increased when WO_3 thin films sputtered on TiO_2. Our previous work [17] found out that the photocatalytic activity of TiO_2 in splitting water was improved to 420 $\mu mol\,L^{-1}\,h^{-1}$ with a suitable amount of WO_3 compounding (optimum concentration was 2%). However, there is no report on TiO_2 modified by Fe, N and WO_3 at the same time.

As a continuous investigation, TiO_2 photocatalysts doped with N, Fe and compounded by WO_3 were composited, and used for photo degradation of formaldehyde solution under the UV-light irradiation in this paper. The Fe element is provided by

* Corresponding author at: Chemical and Biologic Engineering Institute, Changsha University of Science and Technology, Hunan Province Key Laboratory of Materials Protection for Electric Power and Transportation, Changsha 410114, Hunan, China. Tel.: +86 731 85258733; fax: +86 731 85258733.
E-mail address: tonghaixia@126.com (H. Tong).

0925-8388/$ – see front matter © 2011 Elsevier B.V. All rights reserved.
doi:10.1016/j.jallcom.2011.03.068

$Fe(NO_3)_3{\cdot}9H_2O$, which is cheap, nontoxic and simple doping process, and N element is provided by ammonia, which is also cheap, simple doping process and can easily be used practically. Researches on the use of catalysts for photo degradation of formaldehyde under the Vis-light irradiation are in progress.

2. Experimental

2.1. Catalyst preparation

(1) 17 mL butyltitanate was added to 40 mL anhydrous ethyl alcohol drop by drop and then stirred continually for 30 min with magnetic stirrer. A yellow transparent solution was obtained at room temperature, and was titled A.
(2) 10 mL glacial acetic acid was added to 5 mL distilled water, and then shaked the mixture up, and added to 40 mL ethanol. Solution B was obtained.
(3) Solution A was dropwise added to solution B under vigorous stirring at room temperature, and then adjusted pH value to 1–2 with concentrated hydrochloric acid. When the color of the solution turned to light yellow, continue to stir for half an hour.
(4) After aging at room temperature for 24 h, the obtained sol solution was dried at 40 °C until a dry gel was gotten. This gel was grinded and calcined in air for 4 h at 500 °C, with a constant heating rate of 1 °C min^{-1}. After grinded for 1 h, crystalline TiO_2 particles was obtained, and denoted as: T(0).

In step (3), before the pH adjustment, 10 drops of stronger ammonia water were added and other steps were unchanged. At last the N doped TiO_2 was obtained, and denoted as: T(N); different amounts of $Fe(NO_3)_3{\cdot}9H_2O$ solid was dissolved in the appropriate anhydrous ethanol, and added into the mixture before the ammonia water, and other steps were unchanged. At last a series of N, Fe co-doped TiO_2 catalysts: N–0.1% Fe–TiO_2, N–0.5% Fe–TiO_2, N–0.7% Fe–TiO_2, N–1.0% Fe–TiO_2 were obtained, and denoted as: T(NF1), T(NF2), T(NF3), T(NF4), respectively.

The prepared N–0.5% Fe–TiO_2 (T(NF2)) powder was immersed in different concentrations of APT (ammonium paratungstate) solution, and grinded for half an hour, then dried in an infrared oven for 2 h at 100 °C. After grinded for half an hour, the mixture was calcined at 500 °C for 4 h, and then cooled to room temperature; grinded and the powders of N–0.5% Fe–xWO_3–TiO_2 catalyst were obtained, and the value of x was 0.5%, 1%, 2%, 4%, 6%, respectively, the catalyst powders were denoted as: T(NFW1), T(NFW2), T(NFW3), T(NFW4), T(NFW5), respectively.

2.2. Characterization of photocatalysts

X-ray diffraction analysis (XRD) was used to check the coexistence of different crystal phases of the catalyst by a HATCHI D/max2250 powder X-ray diffractometer. The diffraction profiles were recorded with Cu $K\alpha_1$ radiation (0.154056 nm) over a 2θ range of 10–90°. A plumbaginous counter with monochromator was used. The X-ray tube was operated at 40 kV and 300 mA.

X-ray photoelectron spectroscopy (XPS) was recorded on an ESCALAB 250 spectrometer. The monochromatized Al Kα X-ray source was operated at 12 kV and 20 mA.

Diffuse reflectance UV–Vis spectra (UV-DRS) measurements were carried out on a Beijing Purkinje TU-1901 UV/Vis spectrophotometer equipped by a diffuse reflectance accessory with an IS19-1 integrating sphere, and $BaSO_4$ powder was used as reference.

Surface morphology of the TiO_2 catalysts was examined by scanning electron microscope (Japan JSM-5600LV). Small pieces of the prepared photocatalysts were stuck on stubs using double-sided tape. Before the samples were analyzed, they were sputtered with a layer of gold film to prevent the occurrence of charging effect.

2.3. Photocatalytic degradation of formaldehyde

The photocatalytic activity of the TiO_2 catalysts was studied by degradation of formaldehyde as a target pollutant. The experiments were carried out in a 250 mL cylindrical glass reactor inside equipped with an ultraviolet (UV) lamp (365 nm, 250 W) using 250 mL formaldehyde solution with an initial concentration of 30 μg/mL and 0.5 g catalyst. Before the photocatalytic degradation, the suspension was magnetically stirred in the dark for 30 min to establish a formaldehyde adsorption/desorption equilibrium. 5 mL solution was collected from the suspension and was immediately centrifuged at 4000 rpm for 10 min. The concentration of formaldehyde was determined by spectroscopic analysis at 270 nm using a TU-1900 UV spectrometer (Beijing Purkinje General Instrument Co. Ltd., China). The corresponding formaldehyde degradation rate was calculated according to the following equation:

$$\eta = \frac{A^0 - A}{A^0} \times 100\% \quad (1)$$

where A^0 is the initial concentration pollutant, A is the concentration of model pollutant at experimental time t.

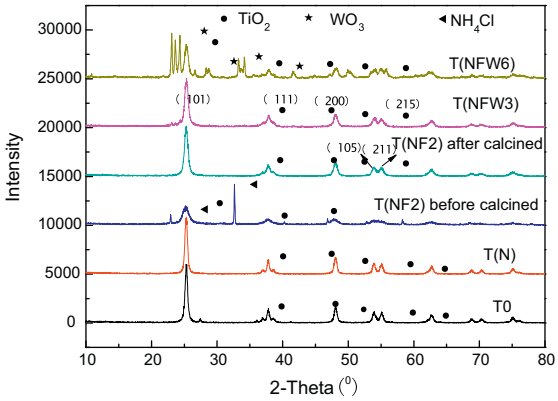

Fig. 1. XRD patterns of TiO_2 catalysts.

3. Results and discussion

3.1. Crystal structure and morphology of TiO_2 catalysts

XRD analysis was carried out to confirm the polymorphs and crystalline phases of TiO_2 catalysts. The XRD patterns for the modified TiO_2 catalysts are shown in Fig. 1. From Fig. 1 the diffraction peaks locating at $2\theta = 25.26$, 37.8 and 48.0° could assign to the planes of (101), (111) and (200), respectively, all of which match well with the anatase TiO_2. After N doping, compared with pure TiO_2, the lattice parameter in c-axils increased (c = 9.4553 and 9.4994 nm for T(0) and T(N), respectively), suggesting N had inserted into the crystal lattice of TiO_2. The patterns of T(NF2) before calcined show that the diffraction peaks locating at $2\theta = 23.24$ and 33.8°, all of which match well with the spectra of NH_4Cl. The peaks of NH_4Cl phase disappeared after calcined at 500 °C for 4 h, which also indicated that N had entered into TiO_2 lattice. In order to confirm the result of N doping into TiO_2 from other aspect, the XPS result of T(N) is shown in Table 1. From Table 1 the content of N is about 1.07%.

On the other hand, before and after calcined, no peak of Fe_2O_3 was found in the XRD pattern of T(NF2) since small amount of iron ions were added.

There is no characteristic diffraction peak of WO_3 and other tungsten oxide phase exist in the pattern of T(NFW3), and it was found in the pattern of T(NFW6). WO_3 can be well dispersed on the TiO_2 phase when its concentration is less than 2%, but gathered and crystallized when the concentration is more than 2% [16], which can be expressed clearly according to the XRD pattern.

SEM images of the catalysts at magnification of 30,000 and 5000 times are shown in Figs. 2 and 3, respectively. From the SEM images the catalysts powder agglomerates significantly. Fig. 2 shows that T(NF1) is sculptured "pattern" compared with other powders, while the T(NF4) in the "pattern" is less clear than that of T(NF1). Viewed the SEM of 5000 times, the spherical morphology of T(NF1) powder is obvious; viewed from Fig. 3 T(0) and T(N) agglomerate significantly less serious than that of Fe-doping and WO_3 compounding TiO_2 powders, which indicates that Fe^{3+} doping can reduce the particle size. To understand the role of WO_3 compounding on the particle size needs further verification because that WO_3 compounding TiO_2 photocatalysts were grinded twice, which can reduce the particle size.

3.2. UV-DRS analysis

The DRS results of the catalysts with different Fe^{3+} contents are shown in Fig. 4. The experimental results indicated that the

Table 1
XPS result of sample N–TiO_2.

Name	Start BE	Peak BE	End BE	Height counts	FWHM (eV)	Area (P) (CPS eV)	Area (N)	At.%
Ti2p3	461.35	458.56	456.15	13,143.44	1.05	15,652	0.07	27.54
N1s	403	399.73	397.05	148.57	0.28	210.86	0	1.07
O1s	533.85	529.77	527.55	14,149.38	1.24	22,537.73	0.18	71.39

undoped TiO_2 powder (T(0)) shows strong photoabsorption only at wavelengths shorter than 400 nm, which is the characteristic absorption of the charge transfer of O2p → Ti3d resulted from the charge transfer from oxygen atom coordinated with titanium to the empty orbit of the center titanium atom [18]. While Fe^{3+} and N-doped TiO_2 nanoparticles show photoabsorption in visible region and the absorption edge shifts to a longer wavelength. With the same N-doped contents, the shift of the reflectance spectrum is due to increasing Fe^{3+} contents. This indicates a decrease in the band gap of TiO_2.

Fig. 5 shows the reflectance spectra of T(0), T(NF2) and T(NF2) with different WO_3 compounding. Obviously, the absorption of T(NF2) with different WO_3 compounding larger than that of T(0), T(NF2) nanoparticles in the visible rigion. With the increase of compounding WO_3 concentration, T(NF2) catalysts exhibit wider optical absorption, and the absorption order is T(NFW1) < T(NFW2) < T(NFW3) < T(NFW5) in the visible region, and who were grinded twice. So besides the particle size, WO_3 compounding can make the absorption of TiO_2 red shift. It is because coupled WO_3 can introduce an impurity level between the valence

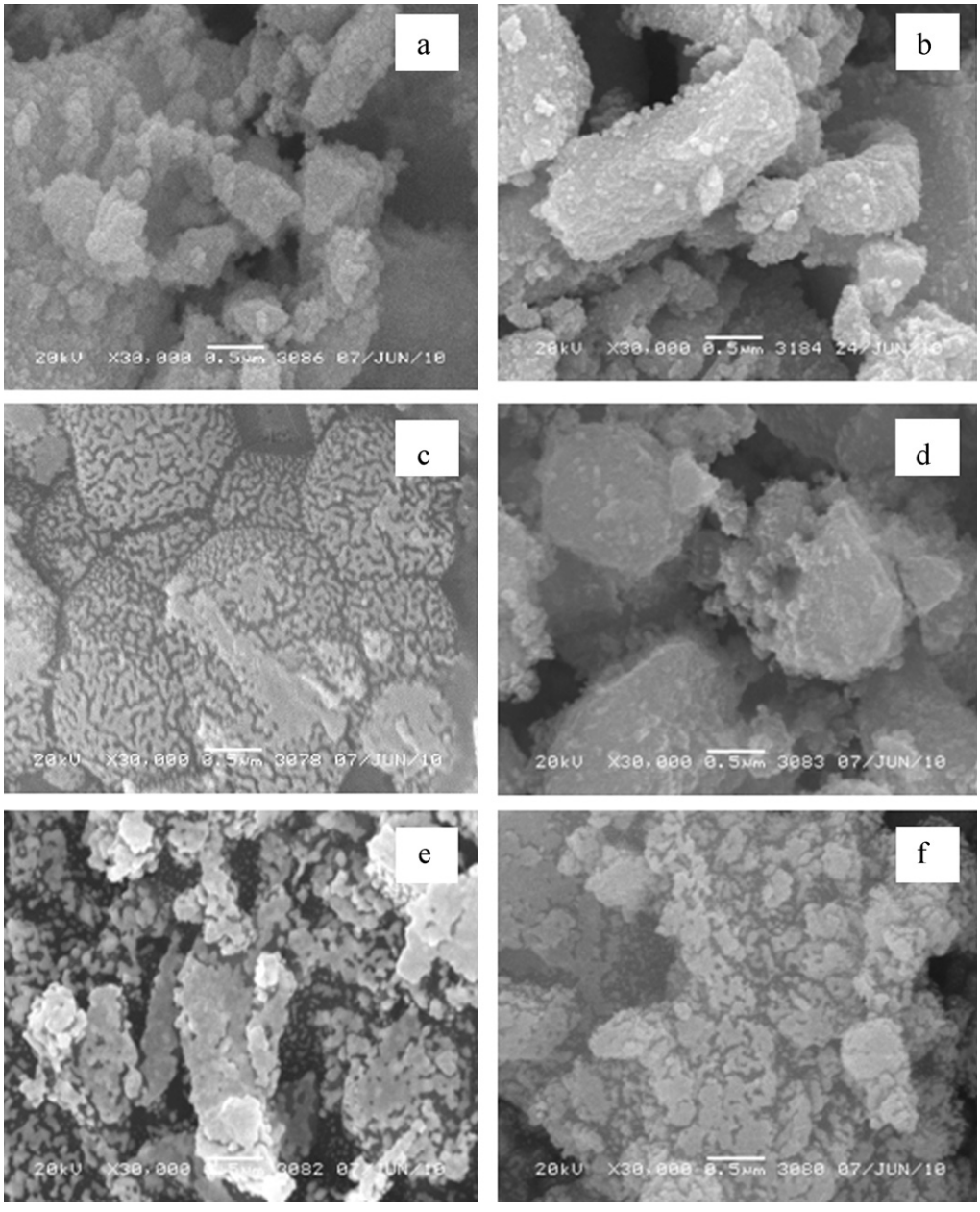

Fig. 2. SEM images of TiO_2 photocatalysts magnified 30,000×. (a) TiO_2, (b) N–TiO_2, (c) N–0.1% Fe–TiO_2, (d) N–0.5% Fe–2% WO_3–TiO_2, (e) N–0.5% Fe–1% WO_3–TiO_2, (f) N–1.0% Fe–TiO_2.

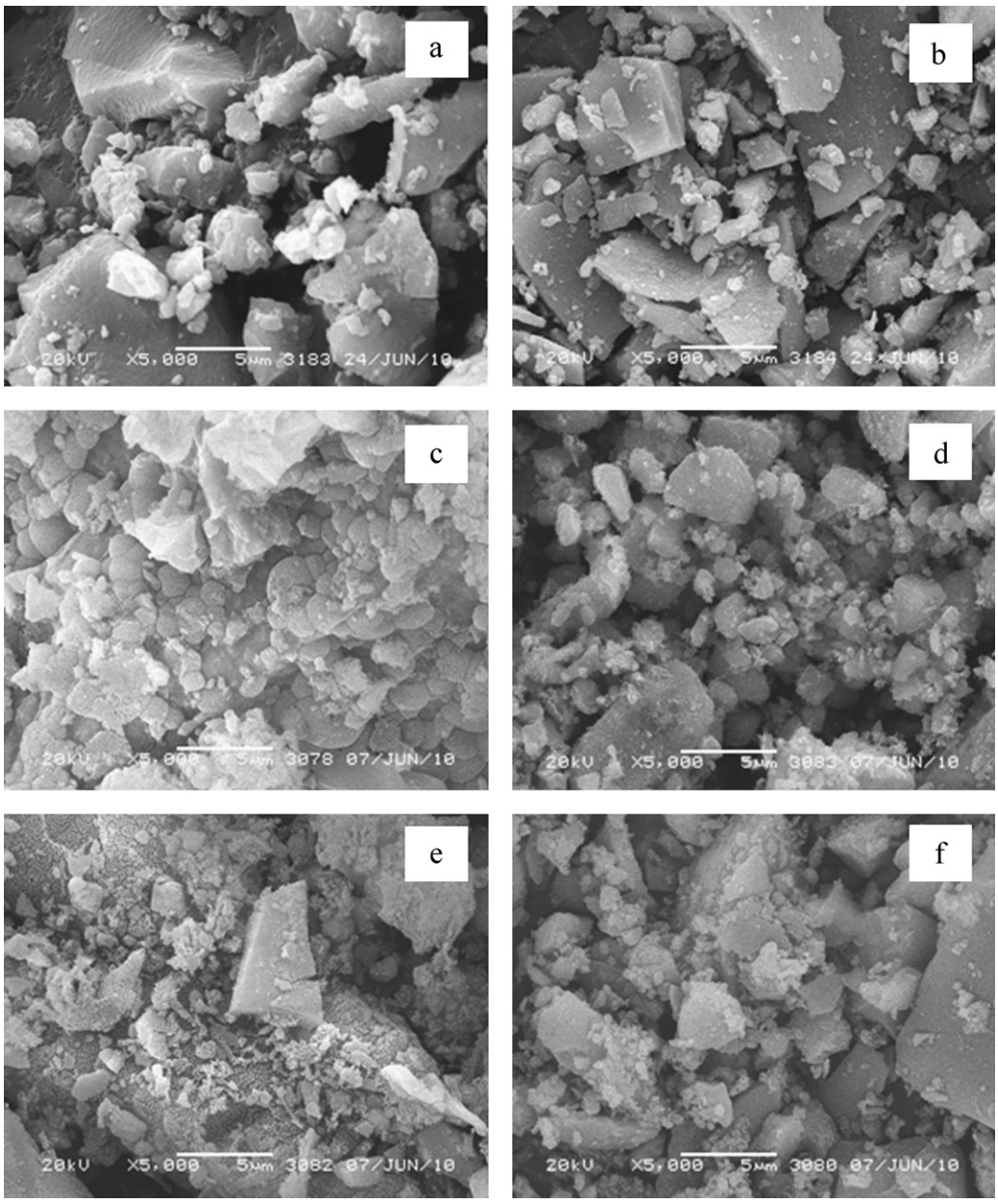

Fig. 3. SEM images of TiO_2 photocatalysts magnified 5000×. (a) TiO_2, (b) N–TiO_2, (c) N–0.1% Fe–TiO_2, (d) 0.5% Fe–N–2% WO_3–TiO_2, (e) N–0.5% Fe–1% WO_3–TiO_2, (f) N–1.0% Fe–TiO_2.

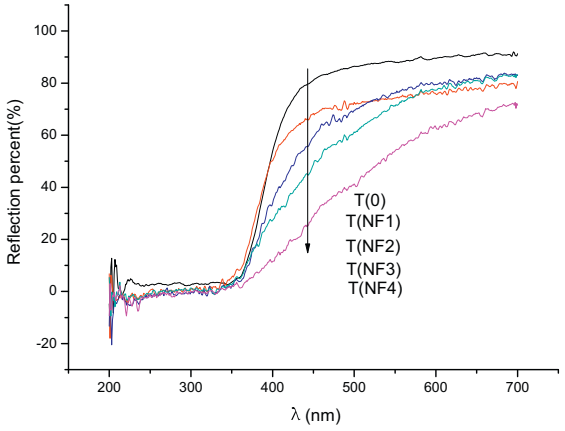

Fig. 4. UV-DRS of catalysts with different Fe^{3+} doping.

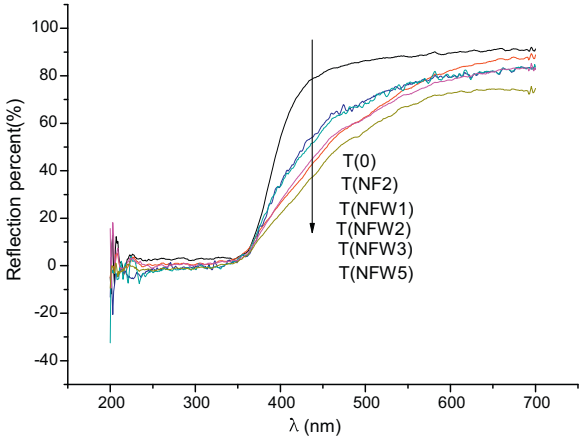

Fig. 5. UV-DRS of catalysts with different WO_3 compounding.

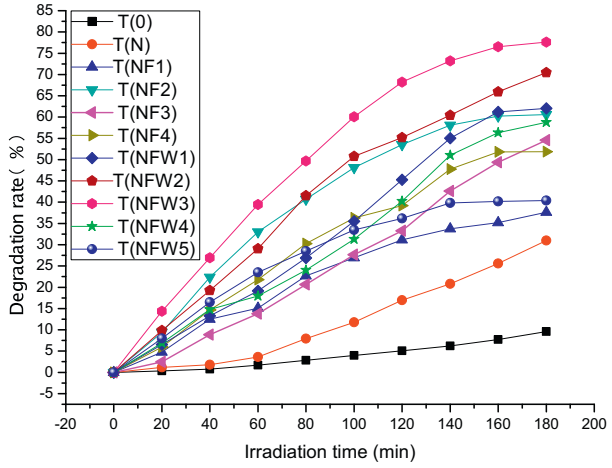

Fig. 6. Photocatalytic degradation of CH_2O by pure TiO_2 and modified TiO_2 catalysts.

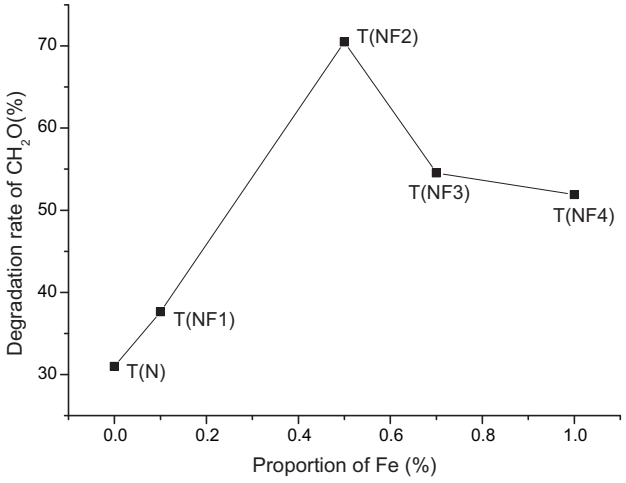

Fig. 7. The dependence of Fe doping concentration and the degradation rate of CH_2O.

and conduction band of TiO_2 and decrease its band gap [19].

3.3. Photocatalytic activity investigation

To evaluate the photocatalytic activity of the N and Fe-doped TiO_2 photocatalysts, degradations of CH_2O solution were run under UV irradiation which are graphically illustrated in Fig. 6. According to literature [20], there is almost no effect on the degradation of CH_2O by UV alone, so formaldehyde degradations are due to TiO_2 photocatalysts. From the figure, N and Fe-doped TiO_2 exhibits much greater activity than that of pure TiO_2. Fig. 7 reflects the photocatalytic activity of TiO_2 photocatalysts with different Fe contents and same N content. The experiment results indicate that the photocatalytic activity of TiO_2 photocatalysts with same N content can be improved by doping an appropriate content of Fe. When the Fe content is 0.5 mol%, the photocatalyst exhibits higher photocatalytic activity. If the Fe content continuously increases, the photocatalytic activity begins to fall down inversely. The degradation rates of T(N), T(NF1), T(NF2), T(NF3) and T(NF4) are 30.99%, 37.635%, 60.57%, 54.54% and 51.885%, respectively.

The photocatalytic activities of T(NF2) photocatalysts with different WO_3 compounding are shown in Fig. 6, and the relationship between WO_3 concentration and the CH_2O degradation rate is shown in Fig. 8. During the degradation process for 3 h, the degradation rate for T(NFW1), T(NFW2), T(NFW3), T(NFW4) and T(NFW5) are 62.055%, 70.47%, 77.61%, 58.785% and 40.38%, respectively. It

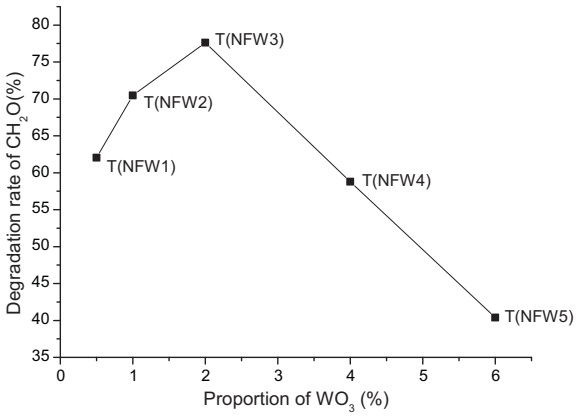

Fig. 8. The dependence of WO_3 compounding concentration and the degradation rate of CH_2O.

is easy to conclude that the optimize concentration of WO_3 compounding is 2 mol%, which is consistent with the reported result [16,17].

During the calcination process N and TiO_2 can form $TiO_{2-x}N_x$, and a new energy band which narrows the band gap of TiO_2 has been introduced in. The doping band introduced from the mixture of substitutional N2p and O2p orbits is responsible for the gap narrowing [21].

When it comes to the impact of doping Fe^{3+}, it generally considers that Fe^{3+} can capture photoproduced electrons, and reduces the probability of electrons and holes to recombination and extends the average life expectancy of the holes, which is beneficial to improve the photocatalytic activity [22]. In addition, the study also shows that Fe^{3+} can be e-captured, due to the facts that the energy levels for Fe^{2+}/Fe^{3+} and Ti^{3+}/Ti^{4+} are close, and thus the capturing electron is easy to migrate to the neighboring Ti^{4+} and then to the solid surface [23]. When the content of Fe was lower than its optimal ratio, Fe would be a separation center. When the content of Fe was higher than its optimal ratio Fe would be are combination center, there by the photocatalytic activity decreased.

Scholz et al. [24] applied the photoelectron spectroscopy method and detected that: when WO_3 disperses on the surface of TiO_2, and the mass fraction of W is about 3.8%, and the single distribution coefficient for WO_3 on the surface of TiO_2 is 1.11. It can be calculated that the mole fraction of WO_3 to TiO_2 is about 2%. It means that tungsten oxide will form a single molecular layer on the TiO_2 surface when the mole fraction of WO_3 to TiO_2 is about 2%. Appropriate amount of WO_3 compounding may promote the separation of photoproduced electron–hole pairs and the transportation of carrier effectively, and improve the photocatalytic activity of the catalyst. However, when the excessive WO_3 on the surface of TiO_2 the transfer center will become an electronic recombination center, and it would reduce the separation efficiency of the photoproduced electrons and holes, and photocatalytic activity of TiO_2 reduces [25].

Researches on the photocatalytic properties of the catalysts under visible light irradiation will be carried out in the future.

4. Conclusion

N, Fe^{3+} doped and WO_3 compounding TiO_2 particles have been synthesized and characterized. UV–Vis spectra showed that N, Fe^{3+} doping and WO_3 compounding could improve the optical absorbance of TiO_2 catalysts. The optimum doping concentration for Fe^{3+} is 0.5 mol%, and optimum compounding concentration for WO_3 was 2 mol%. Under UV-light irradiation, the maximum CH_2O degradation rate was 77.61%, which was more than 8 times to pure TiO_2 9.608% in 180 min.

Acknowledgements

This project (10CL004) was financially supported by the Hunan Provincial Key Laboratory of Materials Protection for Electric Power and Transportation; project (K-081025) supported by State Key Laboratory Breeding Base of Photocatalysis; Postdoctoral Science Foundation of Central South University.

References

[1] D. Chatterjee, S. Dasgupta, J. Photochem. Photobiol. 6 (2005) 186–205.
[2] V. Augugliaro, M. Litter, L. Palmisano, J. Soria, J. Photochem. Photobiol. 7 (2006) 127–144.
[3] W. Choi, A. Termin, M.R. Hoffman, Angew. Chem. Int. 33 (1994) 1091–1092.
[4] D. Chatterjee, S. Dasguple, J. Photochem. Photobiol. C: Rev. 6 (2005) 185–205.
[5] D. Masih, H. Yoshitake, Y. Izumi, Appl. Catal. A: Gen. 325 (2007) 276–282.
[6] M.M. Mohamed, M.M. Al-Esaimi, J. Mol. Catal. A: Chem. 255 (2006) 53–61.
[7] Z.Q. Liu, Y.C. Wang, W. Chu, Z.H. Li, C.C. Ge, J. Alloys Compd. 501 (2010) 54–59.
[8] D.Y. Wu, M.C. Long, W.M. Cai, C. Chen, Y.H. Wu, J. Alloys Compd. 502 (2010) 289–294.
[9] H. Yang, C.X. Pan, J. Alloys Compd. 501 (2010) L8–L11.
[10] Y.Y. Lv, L.S. Yu, H.Y. Huang, H.L. Liu, Y.Y. Feng, J. Alloys Compd. 488 (2009) 314–319.
[11] S.S. Srinivasan, J. Wade, E.K. Stefanakos, Y. Goswami, J. Alloys Compd. 424 (2006) 322–326.
[12] D.W. Bahnemann, S.N. Kholuiskaya, R. Dillert, A.I. Kulak, A.I. Kokorin, Appl. Catal. B: Environ. 36 (2002) 161–169.
[13] K. Nagaveni, M.S. Hegde, G. Madras, J. Phys. Chem. B 108 (2004) 20204–20212.
[14] N. San, A. Hatipoglu, G. Kocturk, Z. Cmar, J. Photochem. Photobiol. A: Chem. 146 (2002) 189–197.
[15] U. Siemon, D. Bahnemann, J.J. Testa, D. Rodriguez, M.I. Litter, N. Bruno, J. Photochem. Photobiol. A: Chem. 148 (2002) 247–255.
[16] Q. Zhang, X.J. Li, F.B. Li, G.B. Gu, Trans. Nonferrous Met. Soc. China 6 (12) (2002) 1299–1303.
[17] H.X. Tong, Q.Y. Chen, Z.L. Yin, H.P. Hu, Y.H. Yang, Trans. Nonferrous Met. Soc. China 18 (4) (2008) 682–687.
[18] W.X. Zhao, Z.P. Bai, A.L. Ren, G. Bin, X.J. Wang, [J]. Fine Chem. 12 (26) (2009) 1226–1234.
[19] X.Z. Li, F.B. Li, C.L. Yang, W.K Ge, [J]. Photochem. Photobiol. A 141 (2–3) (2001) 209–217.
[20] J.F. Sun, Z.H. Wang, J.Z. Liu, Z.C. Wen, J.H. Zhou, K.F. Cen, J. Environ. Eng. China 3 (3) (2009) 506–510.
[21] L.F. Mei, K.M. Liang, H.E. Wang, Catal. Commun. 8 (2007) 1187–1190.
[22] K.T. Ranjit, B. Viswanathan, J. Photochem. Photobiol. A: Chem. 108 (1997) 79–84.
[23] W. Choi, A. Termin, M.R. Hoffmann, J. Phys. Chem. 98 (1994) 13669–13679.
[24] A. Scholz, B. Schnyder, A. Wokaun, J. Mol. Catal. A: Chem. 138 (1999) 249–261.
[25] H.X. Tong, Q.Y. Chen, Z.L. Yin, H.P. Hu, J. Li, L. Zhao, Trans. Nonferrous Met. Soc. China 4 (18) (2008) 682–687.